Simulation of Microwave Heating of Porous Media Coupled With Heat, Mass and Momentum Transfer

Jiajia Chen[1], Krishnamoorthy Pitchai[2], Sohan Birla[1], Jeyamkondan Subbiah[1,2,*], David Jones[1]
[1]Department of Biological Systems Engineering, University of Nebraska- Lincoln
[2]Department of Food Science and Technology, University of Nebraska- Lincoln
*Corresponding author: 212, L.W. Chase Hall, University of Nebraska-Lincoln, NE, 68583, jeyam.subbiah@unl.edu

Abstract: A microwave heating model coupled with heat, mass, and momentum transfer is needed to fully understand the microwave heating process. In this study a comprehensive 3D model was developed for studying the interaction of microwave with the food. The model includes physics of Maxwell's electromagnetic heating, Fourier's heat transfer, Darcy's momentum transfer, mass conservations of water and vapor, and phase change of water. Predicted spatial and transient temperature profiles were in good agreement with experimental results. The moisture content did not change significantly in both simulation and experiment because of short microwave heating time. A longer heating process and accurate spatial moisture content determination are needed for validating the model further.

Keywords: microwave heating, porous media, heat transfer, mass transfer, momentum transfer

1. Introduction

Microwave heating is rapid and convenient. However, microwave heating of food in domestic microwave oven has the issue of non-uniform heating. The non-uniform heating could lead to serious foodborne illness outbreaks.

Food materials such as whey protein gel, as used in this study, are generally porous media which refers to a solid having void (pore) space that is filled with gas or liquid (Datta, 2007). During the microwave heating process, besides the electromagnetic heating and heat transfer within the food domain, the transport of air and water, the vaporization also can happen within the food materials and on food surfaces, which also will influence the microwave heating performance greatly.

Microwave heating models have been developed to understand the interactions between electromagnetic field with food and packaging materials for improving microwave heating performance. However, most of the models developed (Geedipalli et al., 2007; Pitchai et al., 2012) cannot fully describe the microwave heating process, because these models only considered the electromagnetic heating and heat transfer within the food materials, without coupling mass and momentum transfer. These models can only be used for predicting short time microwave heating processes, where the mass and momentum transfer are not significant. Halder et al. (2007), Rakesh et al. (2012), Warning et al.(2012) have developed multiphase porous media models combining the relevant physics to study microwave combination heating and deep-fat frying processes. Because of the large number of parameters needed in the complex multiphysics model, optimization of the input parameters is still needed to improve the model.

The objective of this study was to develop a comprehensive fully coupled multiphysics model that includes heat, mass, and momentum transfer in model food system. In this article, we elaborated the development of the model and validation of the model with experimental results.

2. Model Development

2.1 Problem Description

When a food product is exposed to microwaves in an oven, the interaction between dielectric food and electromagnetic wave generates heat in the food product. The dissipated heat further is transferred from the hot spots to the cold spots. Meanwhile, the moisture is transported within the product via convection and diffusion process, and moves from the inside of the product to the surface. The moisture vaporizes within the food domain and on the boundary of the product, and diffuses to the air domain of the microwave oven resulting in heat loss due to vaporization.

2.2 Governing Equations

2.2.1 Electromagnetics

Electromagnetic field (**E**) at any point in the computational domain is governed by set of Maxwell's equations. The combined wave form of Maxwell's equation is expressed as (COMSOL, 2011):

$$\nabla \times \mu_r^{-1}(\nabla \times \mathbf{E}) - (\frac{2\pi f}{c})^2(\varepsilon_r - i\varepsilon'')\mathbf{E} = 0 \quad (1)$$

where f is frequency (2.45 GHz), c is the speed of light (3×10^8 m/s), ε_r, ε'', and μ_r are relative dielectric constant, dielectric loss factor, and permeability of the medium, respectively.

Electromagnetic power dissipation density (Q) is the function of frequency, loss factor (ε''), and electric field strength:

$$Q = 2\pi f \varepsilon_0 \varepsilon'' \mathbf{E}^2 \quad (2)$$

2.2.2 Mass Conservation

For the conservation of mass, the governing equation for water and vapor transport within the product is given by:

$$\frac{\partial c_i}{\partial t} + \nabla \cdot (-D_i \nabla c_i) + \mathbf{u} \cdot \nabla c_i = \dot{I} \quad (3)$$

where c is the concentration of the species (water and vapor), D denotes the diffusion coefficient, $\dot{I}$ is the water vaporization rate) for the species, **u** is the velocity vector.

2.2.3 Momentum Conservation

The momentum balance of fluid is governed by Darcy's Law. The velocity field (**u**) is determined by:

$$\mathbf{u} = -\frac{k}{\mu}\nabla p \quad (4)$$

where k is the permeability of porous media, μ is the dynamic viscosity of the fluid, p is the pressure.

The Darcy's Law combining with the continuity equation can be written as:

$$\frac{\partial}{\partial t}(\rho \emptyset) + \nabla \cdot (\rho \mathbf{u}) = Q_m \quad (5)$$

where ρ is the density of fluid, ϕ is the porosity, and Q_m is a mass source term. Porosity is defined as the fraction of the control that is occupied by pores, which can vary from zero for pure solid regions to unity for domains of free flow.

2.2.4 Energy Conservation

Energy conservation includes convection, diffusion, conduction, phase change of water and microwave heating source, which can be described by:

$$(\rho C_p)_{eff}\frac{\partial T}{\partial t} + \rho C_p \mathbf{u} \cdot \nabla T = \nabla \cdot (k_{eff} \nabla T) + Q \quad (6)$$

where ρ is the fluid density, C_p is the fluid heat capacity, **u** is the fluid velocity field, Q is the heat source of electromagnetic power dissipation density, $(\rho C_p)_{eff}$ and k_{eff} are the effective heat capacity and thermal conductivity, respectively, which are weighted average of solid-fluid system terms.

2.2.5 Phase Change (Water Vaporization)

The phase change of water (vaporization) is described using non-equilibrium evaporation method because of the easy implementation in commercial software (Halder et al., 2007):

$$\dot{I} = K(\rho_{v,eq} - \rho_v) \quad (7)$$

where $\rho_{v,eq}$ is the equilibrium vapor density, K is a parameter signifying the rate constant of vaporization, which is of the order of 1 for hygroscopic material estimated by Halder et al., (2007).

2.3 Boundary Conditions

The wall of the oven was assumed to be a perfect electrical conductor, where electric field strength **E** is zero.

For the boundaries of food surfaces, the governing heat transfer equation is solved using:

$$-n \cdot (-k\nabla T) = q_{evp} + h(T_{air} - T) \quad (8)$$

where q_{evp} is the heat loss due to vaporization.

The pressure of food boundaries was set to ambient:

$$P|_s = P_{amb} \quad (9)$$

2.4 Geometric Model

Geometric model was developed for an 1100 W Panasonic microwave oven (NNSD767W). In the geometric model, oven cavity, magnetron, turntable, waveguide, crevices and a metal bump are included, as shown in Figure. 1. Microwaves are fed into the cavity through a waveguide located on the right side of the cavity wall. The magnetron was included as a co-axial microwave power source.

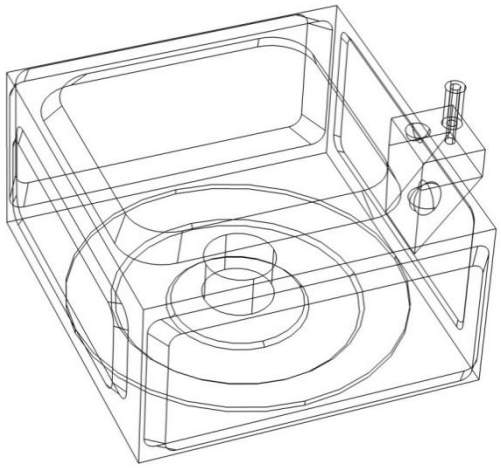

Figure. 1 Geometric model of microwave oven.

2.5 Assumptions

In this study, the following assumptions were made to simplify the model.

a) The microwave frequency was assumed to be constant, i.e. 2.45 GHz.

b) The air temperature was assumed to be constant of 20 °C.

c) There is no bound water in the food domain, which means there is no shrinkage after water vaporization.

d) The initial distribution of water content and temperature are uniform.

2.6 Simulation Strategy

The whole domain was discretized in tetrahedral elements, and size of the elements in different domain was selected to meet 10 linear elements per wavelength criterion (COMSOL, 2011). For food domain, 6 mm maximum element was found to be the optimal mesh size. The entire discretized domains consisted of 82,574 tetrahedral elements. An iterative GMRES solver was used for calculating electromagnetic field. A direct segregated solver was used for solving all other dependent variables and updated electromagnetic field for every time step because of the temperature dependent material properties. The simulations were performed on a 2.4 GHz windows workstation with 48 GB memory and took about 13 hours for 60 s heating simulation.

Various input parameters used in the simulations were obtained from literatures (Rakesh et al., 2012). The dielectric properties were measured using an open-ended coaxial probe method as a function of temperature. Thermal conductivity was measured using KD-2 Pro thermal properties analyzer (Decagon Devices, Inc., Pullman, WA) connected with a single-needle (KS-1 6 cm sensor). The specific heat capacities of whey protein gel were measured by Mettler Differential Scanning Calorimeter (Mettler Toledo, DSC 822) as a function of temperature at the heating rate of 2 °C/min.

2.7 Experimental Validation

Cylindrical samples of whey protein gel were used to validate the model. Whey protein gel was formed by dissolving 20% whey protein powder (80% concentrate), 0.56% $CaCl_2$ and 0.5% guar gum in deionized water. The model food was subjected to microwave heating for 60 s, while the food was kept on stationary glass turntable. Transient temperatures at four points as shown in Figure. 2 were recorded using fiber-optic sensors (4-channel reflex signal conditioner, accuracy ±0.8°C, Neoptix Inc., Quebec, Canada). Immediately after completion of the heating, the thermal images of top and bottom of gel cylinder were taken using a thermal imaging camera (SC640, accuracy ±2°C, 640× 480 pixels, FLIR systems, Boston, MA). Then, the sample was sliced horizontally in the middle (25 mm from top) to obtain image at the middle plane. The moisture contents at different locations were also determined.

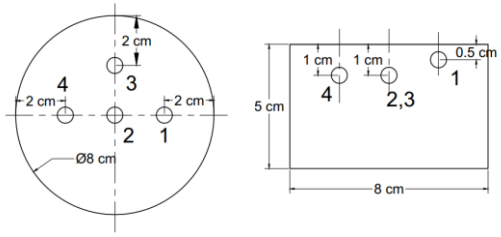

(a) Top view (b) Front view

Figure. 2 Locations of fiber optic sensors used for monitoring transient temperature in model food.

3. Results and Discussions

3.1 Predicted and Experimental Spatial Temperatures Profiles

Figure. 3 shows the comparison of predicted and experimental spatial temperature profiles at top, middle and bottom layers of model food after 60 s microwave heating. The

predicted spatial temperature patterns (hot and cold spots) show a good agreement with the observed spatial temperature profiles. All the predicted temperature ranges of three layers were higher than those of experimental results, which are partly attributed to the heat loss during the thermal images acquisition process in experiment. There was a variation in heating between predicted spatial temperature profiles and experimental results.

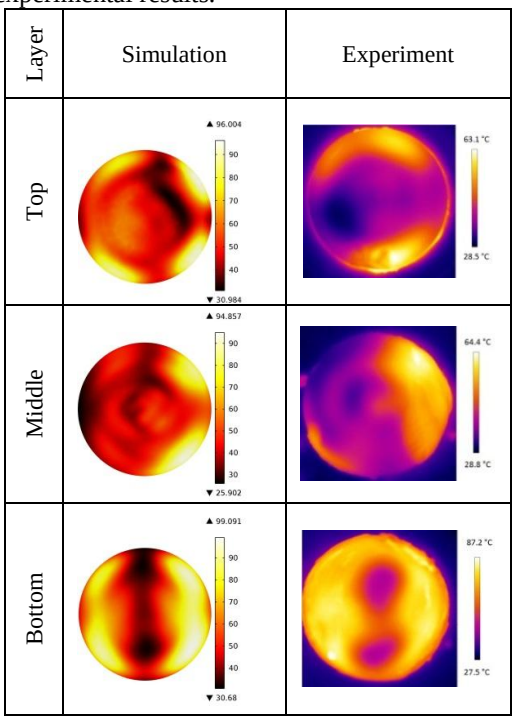

Figure. 3 Predicted and observed spatial temperature profiles at three layers.

3.2 Predicted and Experimental Transient Temperature Profiles

Figure. 4 shows a comparison between predicted and observed transient temperature profiles at four locations as shown in Figure. 2. It shows that the predicted result has good agreement with the experimental data at point 1 and point 2. The predicted and observed transient temperature profiles of point 1 and point 2 followed the similar trend. The RMSE of the profiles of point 1 and point 2 are 1.1 and 0.7 °C, respectively. However, there was still large deviation for points 3 and 4, as the RMSE values are 2.7 and 6.0 °C, respectively, which may be due to the slightly different initial temperatures and mismatch locations between simulation and experiment.

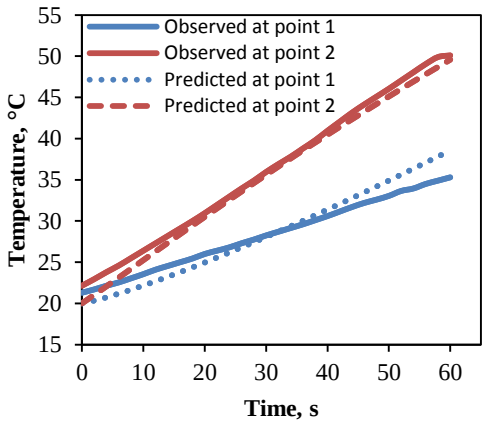

(a) Point1 and Point 2

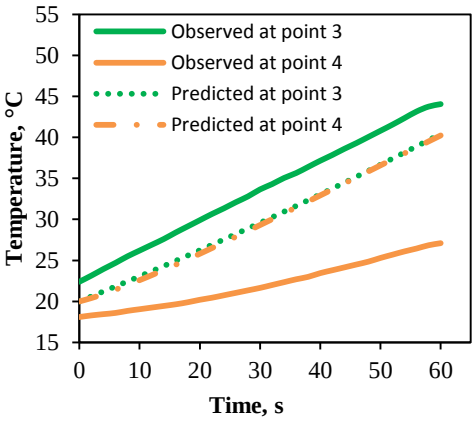

(b) Point 3 and Point 4

Figure. 4 Predicted and observed transient temperature heating profiles at four locations. (a) point 1 and point 2 (b) point 3 and point 4 Description of locations of points is provided in Figure. 2.

3.3 Moisture Content

After 60 s microwave heating, the volume moisture contents of the food sample changed very little as shown in Figure. 5, from the initial value of 80% to the final values of 79.24% to 79.96%, which was also found in the experiment. The experimental initial and final moisture contents were both (80.1±0.1)% (weight base). Granted, the model food was only heated for a short time. Heating processes with longer durations and accurate spatial moisture content measurement are needed to further validate the models. Further studies are underway to validate the model for longer time.

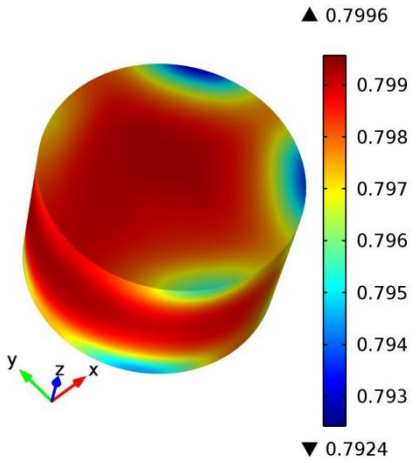

Figure. 5 Predicted volume moisture content (kg water/kg sample).

Figure. 6 shows a comparison between predicted spatial temperature profiles and moisture content profiles. It shows that the predicted moisture content profile has a good agreement with temperature profile. Although moisture content did not show great difference in the range, the relative lower moisture content locations matched with the higher temperature locations, which is due to the more water vaporization in the higher temperature areas.

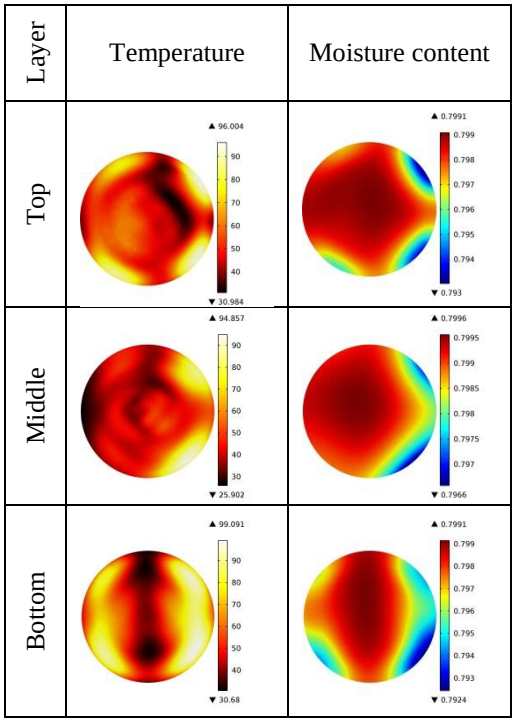

Figure. 6 Predicted spatial temperature profiles and moisture content profiles.

4. Conclusions

A comprehensive model of microwave heating coupled with heat, mass, and momentum transfer was developed to study the interaction between electromagnetic waves and a model food. The predicted spatial and transient temperature profiles showed good agreement with experimental results. There was variation between predicted and experimental temperature scale. Due to short heating time, moisture content did not change greatly. The longer heating process and accurate spatial moisture content measurement are needed to further validate the models.

5. Acknowledgements

The authors acknowledge the financial support provided by ConAgra Foods, Inc.

6. References

1. COMSOL, COMSOL user guide on RF module, (2011).
2. Datta, A.K., Porous media approaches to studying simultaneous heat and mass transfer in food processes. I: problem formulations, *Journal of Food Engineering*, **80**, 80-95 (2007).
3. Geedipalli, S.S.R., Rakesh, V., and Datta, A.K. Modeling the heating uniformity contributed by a rotating turntable in microwave ovens. *Journal of Food Engineering*, **82**, 359-368 (2007).
4. Halder, A., Dhall, A., and Datta A.K., An improved, easily implementable, porous media based model for deep-fat frying, Part I: model development and input parameters, *Food and Bioproducts Processing*, **85**, 209-219 (2007).
5. Pitchai, K., Birla, S.L., Subbiah, J., Jones, D. and Thippareddi, H., Coupled electromagnetic and heat transfer model for microwave heating in domestic ovens, *Journal of Food Engineering*, **112**, 100-111 (2012).
6. Rakesh, V., Datta, A.K., Walton, J.H., McCarthy, K.L., and McCarthy, M.J., Microwave combination heating: coupled electromagnetics-multiphase porous media modeling and MRI experimentation, *Bioengineering, Food, and Natural Products*, **58**, 1262-1278 (2012).
7. Warning, A., Dhall, A., Mitrea, D., and Datta, A.K., Porous media based model for deep-fat vacuum frying potato chips, *Journal of Food Engineering*, **110**, 428-440 (2012).